

Geometric scaling effects on instrumental plate height in field flow fractionation

Himanshu J. Sant^{a,*}, Bruce K. Gale^{b,1}

^a *Utah State Center for Biomedical Microfluidics, Department of Bioengineering, University of Utah, 50 S. Central Campus Drive, Rm#2480, Salt Lake City, UT 84112, USA*

^b *Utah State Center for Biomedical Microfluidics, Department of Mechanical Engineering, 50 S. Central Campus Drive, Rm#2110, Salt Lake City, UT 84112, USA*

Received 25 July 2005; received in revised form 24 November 2005; accepted 29 November 2005
Available online 20 December 2005

Abstract

This paper examines geometric scaling models for field flow fractionation systems to understand how channel dimensions affect resolution and retention. Specifically, the changing contribution of the instrumental plate height during miniaturization of field flow fractionation (FFF) systems is reported. The work is directed towards determining the optimal geometrical parameters for miniaturization of field flow fractionation systems. The experimental relationship between channel height in FFF systems and instrumental plate heights is reported. FFF scaling models are modified to: (i) better clarify the dependence of plate height and resolution on channel height in FFF and (ii) include a more complete geometrical scaling analysis and model comparison in the low retention regime. Electrical field flow fractionation has been shown to benefit from miniaturization, so this paper focuses on that subtype, but surprisingly, the results also indicate the possibility of improvement in performance with miniaturization of other field flow fractionation systems including general FFF subtypes in which the applied field does not vary with channel height. This paper also discusses the potential role of more powerful microscale field flow fractionation systems as a new class of sample preparation units for micro-total-analysis systems (μ -TAS).

© 2005 Elsevier B.V. All rights reserved.

Keywords: Field flow fractionation; Scaling effects; Electrical field flow fractionation; Microfluidic separations; Micro-total-analysis-systems; Instrumental plate height

1. Introduction

A variety of analytical techniques are now available for characterization, analysis, and classification of nanoparticles and biomaterials suspended in liquid media. Typically, these tests are carried out in dedicated labs using large, expensive, slow, and complex equipment. These tools consume large volumes of sample and require a number of different analytical and purification steps. Overall this process considerably delays the desired end result. Accordingly, numerous research groups are working to develop portable versions of laboratory test equipment with the hope of being able to create faster, cheaper, more efficient and

more reliable testing tools. During the last decade this concept has resulted in an explosion of research in the area of micro-total-analysis-systems (μ -TAS) [1,2] or lab-on-a-chip technologies.

Typically, μ -TAS are composed of several unique components that perform specific functions, such as sample preparation, reaction, detection, or signal processing. In such systems, sample preparation is one area that continues to prove difficult to effectively miniaturize. In a μ -TAS the sample preparation system would be used to break down the barriers between the macroscale world of “real” samples and the microscale world of “prepared” samples. Macroscale sample preparation methods are often extremely difficult, complex, or even impossible to implement on the microscale, and may be challenging to fabricate. Therefore, other methods more compatible with micro-fabrication techniques must be developed to allow the full range of lab-on-a-chip devices to be created. One technique that has the potential to address this problem is field flow fractionation (FFF).

* Corresponding author. Tel.: +1 801 585 3176; fax: +1 801 585 9826.

E-mail addresses: himanshu.sant@utah.edu (H.J. Sant), gale@eng.utah.edu (B.K. Gale).

URL: www.mems.utah.edu.

¹ Tel.: +1 801 585 5944; fax: +1 801 585 9826.

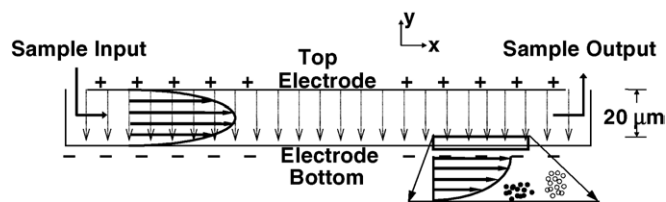


Fig. 1. Diagram of operation of an EIFFF system showing the input and output ports, application of electric field, the parabolic flow profile, the general separation mechanism, and relative channel dimensions.

Field flow fractionation is a chromatography-like separation technique that was first described in the mid-1960s by Giddings [3]. FFF relies on a field perpendicular to the direction of separation to induce a differential migration of particles injected into the system [4]. A wide variety of fields have been used in FFF systems with the most common FFF subtypes being flow [5], thermal [6], sedimentation [7], steric [8], and electrical [9]. Other subtypes of FFF that are of interest include gravitational [10], dielectrophoretic [11], cyclical [12], and magnetic FFF [13]. Combinations of these fields as well as variations on the basic design are commonplace [10,14].

In standard FFF systems, the channel consists of a long, thin, rectangular duct as shown in Fig. 1. Pressure driven flow drives the injected sample plug through the channel and as the sample components interact with the applied field, they are forced towards the wall of the channel. Depending upon the interaction of the different components with the field, they take on a characteristic average distance from the wall. When diffusion opposing the induced movement balances this field-induced movement, an equilibrium condition prevails in the channel. Due to the parabolic velocity profile of the carrier fluid in the channel, the various layers of particles move through the channel at different velocities depending on their protrusion depth into the flow stream.

In the last few years, several microfabricated field flow fractionation systems have been reported including systems that rely on electrical [15,16], thermal [17,18], and dielectrophoretic [19] fields. These systems (along with the macroscale varieties) are now being rapidly developed for a variety of applications including cell and biopolymer characterization and separations, biowarfare agent detection, polymer analysis, and environmental monitoring. One of the promising systems, the electrical field flow fractionation system (EIFFF) [20], has been the subject of recent interest and a recent report elucidated some of the primary scaling advantages associated with miniaturizing the EIFFF system by comparing macroscale and microscale EIFFF system [21]. Miniaturization of all other FFF subtypes may not be as efficient as compared to EFFF, e.g. miniaturized thermal FFF requires higher thermal energy input and efficient cooling in order to achieve a given temperature drop. But there are a number of clear advantages that come from miniaturization of any FFF system [22], including the possibility of on-chip detection and signal processing [23]. Earlier reports [24] have indicated, though, that general FFF systems (those systems in which the applied field does not scale with channel thickness) are unlikely to claim the same scaling advantages associated with thermal

and electrical systems, but this paper will show a few ways in which even general FFF systems may be able to improve performance through miniaturization.

While a recent communication [18] on channel height reduction effects in TFFF seems to indicate the reduced performance with miniaturization for thermal field flow fractionation, the experimental protocol used in that work does not include a reduced sample size, sample injection loop, or post column tubing length as required for successful miniaturized systems. We will discuss the importance of just such instrumental factors in designing a microscale field flow fractionation system in this paper by building on guidelines presented earlier [24,25].

To make μ -TAS practical, the sample preparation systems will need to be both high speed and low power. In FFF theory, high-speed and low retention separations require a more complex analysis than is required for high retention separations that can be modeled accurately using simpler equations. Since high speed and low retention separations will likely be required of FFF systems in a μ -TAS, this work will explore the geometric scaling effects associated with these low retention separations. Therefore, this paper will compare results generated using the best available models [4] and that include additional phenomena such as wall repulsion with the typical approximate expressions that are only valid for high retention [26]. While, a number of publications are available on optimization of the operating conditions for field flow fractionation systems [27], very few communications have attempted to optimize the geometric dimensions of both macroscale and microscale FFF systems, which is the focus of this work.

2. Theory

2.1. Retention

FFF retention theory is generally well developed and provides the framework for the results developed as part of this work [28,29]. A basic parameter in FFF theory is the retention ratio, R , which is defined as the ratio between the elution time (or elution volume) of unretained particles and the retained particles of interest. The retention ratio can be related to the physical parameters of the particles being retained by the equation:

$$R = 6\lambda \left[\coth \left(\frac{1}{2\lambda} \right) - 2\lambda \right] \quad (1)$$

where λ is a non-dimensional parameter related to the thickness, w , of the channel, the applied field strength, and the physical properties of the particles being retained.

At high retention (i.e. low values of R), Eq. (1) for retention ratio is traditionally approximated as,

$$R = 6\lambda. \quad (2)$$

This relationship is accurate within 5% for $R=0.2$, while its accuracy is better than 2% at $R=0.05$ [26]. High speed separations, though, are likely to be produced at retention ratios well above this level (as high as $R=0.7$), so analysis at these lower retention levels needs to be performed to determine whether

miniaturization is still practical at these retention levels. Therefore, this paper will closely compare the theoretical results obtained when Eqs. (1) and (2) are used to estimate performance parameters.

Miniaturization of FFF channels may be limited by particle-wall repulsion effects [20]. These interactions typically result in the exclusion or the repulsion of the particles away from the wall and, hence, reduce the effective retention in FFF channels. These particle-wall interactions include electrostatic forces, hydrodynamic lift, and van der Waal's attractive forces. To correct for these effects and determine their influence, a modified retention parameter is used. Tri et al. [20], have proposed the modification for λ as:

$$\lambda = \frac{l}{w} + \frac{d\gamma'}{2w} + \frac{\delta}{w} \quad (3)$$

where, l is the average particle cloud thickness, d is the diameter of the particles, γ' contains information regarding all external effects other than repulsion and δ is the thickness of exclusion zone. This repulsion effect, which defines a constant exclusion zone, could prove a limitation for miniaturization, so the effect will be included in the retention models used in the discussion of this work. The wall repulsion layer increases the average particle cloud thickness ' l ' and therefore amounts to a change in λ for retention ratio calculations. We have used this modified λ to evaluate the retention ratio in the mathematical calculations.

2.2. Plate height

In the plate theory of chromatography, the length L , of a separation column can be broken down in to N theoretical plates of height H

$$H = \frac{L}{N}. \quad (4)$$

The plate height generally represents the length of the separation column required to generate a defined level of separation between two particles. Thus, H and N can be used as figures of merit for separation systems and allow various instruments to be compared, with the goal being to minimize H and maximize N .

The total plate height can be thought as the sum of several contributing factors such as non-equilibrium effects, H_n , instrumental effects, H_i , polydispersity, H_p and the contribution due to diffusion, H_D [30] as given by:

$$H = H_n + H_i + H_p + H_D. \quad (5)$$

As polydispersity is an inherent property of the sample being processed, it is not a system property and can be ignored when optimizing an instrument. As diffusion coefficients are low for the particles of interest in this work, the contribution of diffusion to plate height is negligible unless very low flow velocities are used. Thus, only the contributions due to non-equilibrium and instrumental effects are taken into consideration during instrument optimization efforts.

2.2.1. Instrumental plate height

In FFF systems, the instrumental component of plate height depends on the instrument set-up, channel geometry, the fluidic connections, post-column volumes, and the sample injection size and method. These elements that contribute to instrumental band broadening are not easily expressed in a comprehensive theory and so have been ignored when examining these systems mathematically and conceptually. Thus, no comprehensive theory of instrumental effects exists and the effect of geometry on instrumental plate height is only known conceptually. Accordingly, in this work we measure the instrumental plate height as a function of FFF channel dimensions and analyze its effect on FFF operation as channel dimensions change.

2.2.2. Non-equilibrium plate height

In FFF, the non-equilibrium component of plate height, H_n , is heavily dependent on channel thickness, diffusion, D and flow velocity, v and is given by:

$$H_n = \frac{\chi(\lambda)w^2\langle v \rangle}{D}. \quad (6)$$

The function $\chi(\lambda)$ is traditionally represented by

$$\chi(\lambda) = 24\lambda^3(1 - 8\lambda + 12\lambda^2). \quad (7)$$

Eq. (7) is a reasonable approximation for $\chi(\lambda)$ with error values of less than 3% for R values up to 0.4 and a maximum error of 9% when R values reach 0.5. Eq. (7) is a much closer approximation to $\chi(\lambda)$ than the simplified form $24\lambda^3$, which was used in earlier publications and has an error of more than 37% for λ about 0.03 ($R=0.2$) [26]. This approximation becomes even poorer as λ gets larger, as will be the case in some high-speed separations. The exact expression for $\chi(\lambda)$ was determined by Giddings [31] and is given by:

$$\chi(\lambda) = 24\lambda^3 \frac{[(28\lambda^2 + 1)(1 - e^{-1/\lambda}) - 10\lambda(e^{-1/\lambda} + 1) - (1/3\lambda^2) - (2/\lambda) + 4 - (1/\lambda)/(1 - e^{-1/\lambda})] \times 4\lambda(1 + (1/\lambda)/(1 - e^{-1/\lambda}) - 1/3\lambda - 6)}{[(1 + e^{-1/\lambda}) - 2\lambda(1 - e^{-1/\lambda})]}. \quad (8)$$

In the results section a comparison of relative effects between the simplified form for $\chi(\lambda)$ and Eq. (8) will be made in an effort to help determine an appropriate choice for geometric scaling models in FFF.

2.3. Resolution

The resolution of a chromatography system, R_s , is a measure of the relative separation ability of a system and can be represented by [15,32]

$$R_s = \frac{\Delta R}{4\bar{R}} \sqrt{\frac{L}{H}}, \quad (9)$$

where ΔR is the difference in retention ratio for two distinct particles and \bar{R} is the average retention ratio of the two particles being considered.

Upon substitution of Eqs. (5) and (6) into Eq. (9), an expression for resolution in FFF takes the form:

$$R_s = \frac{\Delta R}{4\bar{R}} \sqrt{\frac{L\bar{D}}{\chi(\bar{\lambda})w^2\langle v \rangle + \bar{D}H_i}} \quad (10)$$

where \bar{D} represents the average diffusion coefficient for the two particle clouds. An approximate expression, which uses Eq. (2), the relationship $\chi(\lambda) = 24\lambda^3$, and was derived in previous publications [26] can be written as:

$$R_s = \frac{\Delta\lambda}{4\bar{\lambda}} \sqrt{\frac{L\bar{D}}{24\bar{\lambda}^3w^2\langle v \rangle + \bar{D}H_i}}, \quad (11)$$

which is clearly easier to analyze, especially if H_i is assumed to be negligible.

Eqs. (10) and (11) are general FFF equations and can be used for all FFF systems. The geometric scaling effects associated with these equations, though, will vary depending on what type of system is used and whether the field strength is a function of w .

2.4. Length scaling

The channel length in FFF channels can theoretically be of any dimension, but practical considerations such as difficulties in maintaining appropriate tolerances in manufacturing provide some general limitations. A review of the FFF literature indicates that length is typically not an independent variable, but changes in proportion with the channel height, w , especially in systems where the field strength varies with the channel height. Since resolution improves in these systems with miniaturization, the length can be reduced to linearly reduce analysis times [21].

Since L is not a truly independent variable, we have chosen in some analyses to use the following relationship as an estimate of the standard scaling relationship seen in FFF systems

$$L = 3000w. \quad (12)$$

Use of this relationship gives a more reasonable estimate of the true scaling effects in the system when w is reduced and allows the use of just one characteristic dimension, w , for the analysis.

3. Methodology

3.1. Experimental

Standard methods were used to calculate the instrumental plate height and establish a correlation between H_i and w . First, mathematically, the non-equilibrium component of the plate height can be represented by Eq. (6) and is a direct function of flow velocity $\langle v \rangle$. For zero retention, the non-equilibrium component of plate height becomes [31,33]:

$$H_n = \frac{1}{105} \frac{w^2\langle v \rangle}{D}. \quad (13)$$

Since instrumental plate height is assumed to be constant with respect to the flow velocity, on a plot of measured plate height

versus flow rate, the y-intercept (or the extrapolated plate height at zero flowrate) is the instrumental plate height [34].

Experimentally, the instrumental contribution to plate height is estimated by injecting an unretained sample such as acetone into the FFF system and measuring the plate height for a series of flow velocities. To determine the effect of FFF system miniaturization we have used four electrical field flow fractionation channels with channel heights of 254 μm (90 cm long), 178 μm (64 cm long), 127 μm (35 cm long) and 28 μm (6 cm long). For each channel a typical acetone sample was injected using a Hamilton microliter Syringe (10 μL) for a series of flow velocities between 0.5 and 15 mm/s. The injection volumes were 5, 2.5, and 0.1 μL , respectively and correspond to typical injection volumes for those channels. The peaks eluted from 127 to 254 μm channels were detected using an external Linear UV-106 extinction detector monitoring extinction at 254 nm. The peaks in the 28 μm channel were detected using an on-chip conductivity detector [23]. The resulting fractograms were used to estimate the plate height by measuring the width of the sample peak at half height, $w_{1/2}$, and the elution time of the peak, t_r . The number of plates, N , was then be calculated using [34]

$$N = 5.54 \left(\frac{t_r}{w_{1/2}} \right)^2. \quad (14)$$

The total plate height for each sample could then be calculated using Eq. (4) and the instrumental plate height estimated by plotting the measured plate height versus flow rate and finding the y-intercept. The instrumental plate heights were thus determined for each channel and compared to determine any scaling effects.

3.2. Modeling

The basic scaling effects associated with EIFFF systems and some general systems have been presented in earlier papers [21,24], so the results obtained here will be compared to the results presented there. The modeling results obtained for this work were developed using MathCAD software (MathSoft Engineering & Education, Inc., MA) and Table 1 summarizes the values used in the various equations when they were required for comparison. The values were either taken from various FFF publications [26] or from available experimental data [15,24].

Table 1
Values used in mathematical models

| Parameter | Notation | Value |
|---|---------------------|-------------------------|
| Average flow velocity (mm/s) | $\langle v \rangle$ | 1.5 |
| Diameter of particles (nm) | d_1, d_2 | 50, 70 |
| Electrophoretic mobility ($\text{m}^2/\text{V}/\text{s}$) | μ | -1.75×10^{-11} |
| Constant length of the channel (cm) | L | 60 |
| Constant instrumental plate height (μm) | H_i | 600 |
| Thickness of repulsion layer (nm) | δ | 400 |
| Repulsion parameter | γ' | 0.42 |
| Temperature (K) | T | 298 |
| Viscosity of carrier liquid ($\text{N s}/\text{m}^2$) | η | 0.00089 |
| Effective voltage (mV) | V_{eff} | 5 |
| Height of the channel (μm) | w | 10–200 |
| Drift velocity for general FFF (m/s) | U | 1.85×10^{-5} |

Electrical FFF is a unique subtype of the FFF family, due to the electrochemistry involved with application of an electrical field in an aqueous environment. In such a situation, a double layer forms at the electrode surface causing most of the applied voltage to drop across the high-capacitance ionic double layer. Only a fraction (typically 0.5–3%) of total field drops across the bulk of the channel and is used to retain the sample. Due to this low effective field availability, we have used small drift electrophoretic velocity for modeling the electrical FFF system. The modeling was done to determine the impact of the various geometric parameters on the expected performance of the miniaturized systems with the goal of developing knowledge that will allow for improved instrument designs in the future. Models for both EIFFF and general FFF systems are examined and compared to determine what the optimal geometry of these systems may be. Note that all results for plate height and resolution presented in figures are normalized to the highest value of the respective dataset.

4. Results and discussion

4.1. Instrumental plate height

In FFF systems, the instrumental component of plate height is always measured experimentally since it is dependent on the instrument set-up, the connection methods (packaging), and the sample injection size and method. The instrumental plate height data are shown in Fig. 2 and were found to vary linearly with w as determined by a linear fit to the experimental data with a forced zero. The relationship between instrumental plate height and channel height was found to be

$$H_i = 3w. \quad (15)$$

It can clearly be seen that the instrumental plate height drops with a decrease in channel height and subsequent improvement in sample injection, channel fabrication, and detector arrangement [35]. Accordingly, there appears to be a clear advantage to miniaturization with regard to instrumental plate heights.

Before explicitly including the observed variation in instrumental plate height with channel height in the mathematical

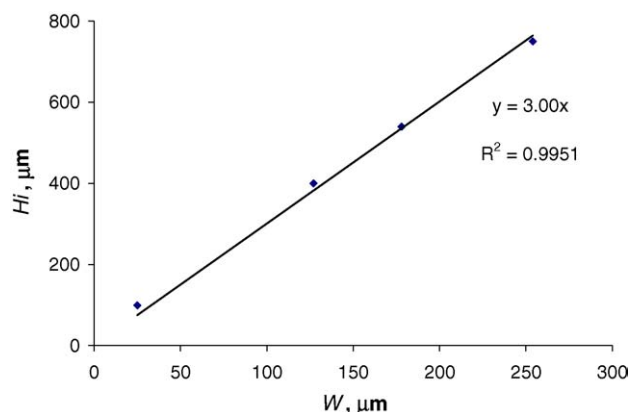


Fig. 2. Plot of measured instrumental plate height, H_i for channel height, w in FFF channels.

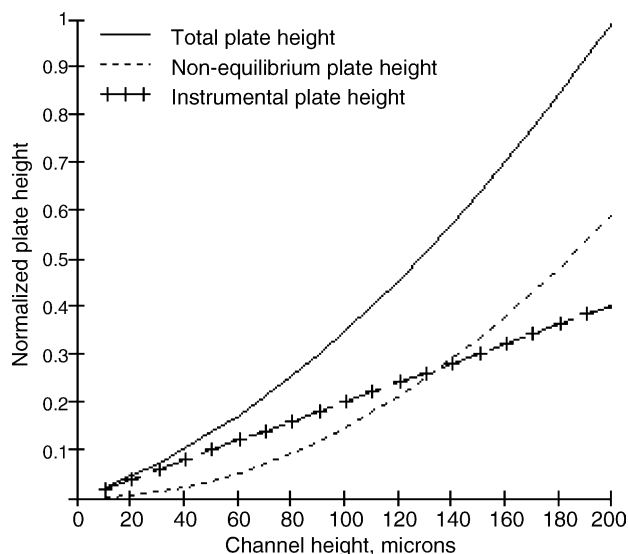


Fig. 3. Plots showing the variation of H_n and H_i with channel height for EIFFF and ThFFF systems (where field strength varies with w).

models and discussing the effect of the instrumental plate height, a brief discussion of geometric scaling will be completed to provide context.

4.2. Plate height scaling

When the relationship in Eq. (15) is used to find the total plate height using Eq. (5) (sum of non-equilibrium and instrumental plate heights) for FFF systems as shown in Figs. 3 and 4, we see a clear difference in the relative importance of non-equilibrium and instrumental contributions of the plate height.

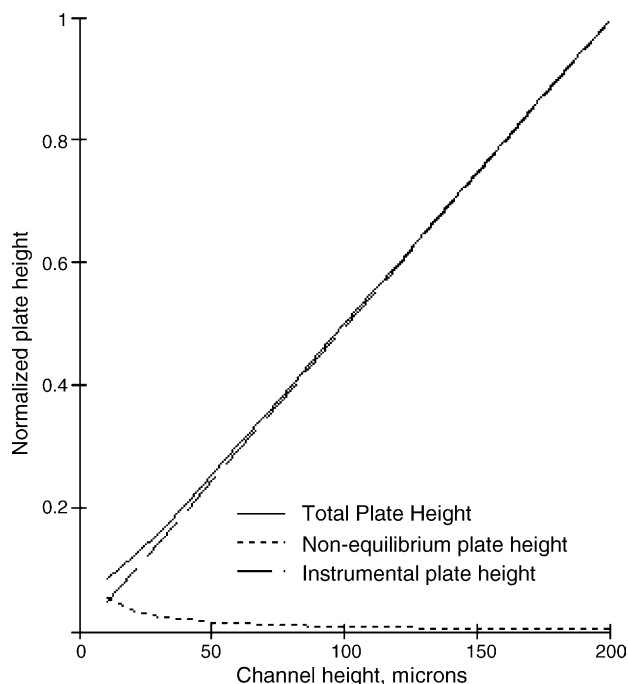


Fig. 4. Plate height variation for general FFF systems (where field strength is independent of w).

Fig. 3 shows the estimates for EIFFF systems, which indicate that plate heights are dominated by non-equilibrium effects, which generate an exponential increase in plate height as w increases. In EFFF the non-equilibrium plate height is a strong function of the applied field. In fact at 0.25% effective field strength, non-equilibrium plate height is 10 times higher than the instrumental plate height, but as field strength is increased to 1.25%, the relative magnitudes of the instrumental and non-equilibrium contributions are similar. It should be noted here that a change in effective field from 0.25 to 1.25% results in a retention ratio change from 0.069 to 0.016 (corresponding to a change in retention time of 10–40 min for a 40 s void time). Fig. 4 shows the relative contributions to plate height for general FFF systems (such as flow FFF, sedimentation FFF, magnetic FFF, gravitational FFF, and others), and demonstrates how the relative importance of non-equilibrium and instrumental effects has switched. In this case the non-equilibrium effect is almost negligible and the plate height is dominated by instrumental effects. This dependence on instrumental effects will be very important when we discuss the overall impact of miniaturization later in this work.

4.3. Resolution models

By substituting Eqs. (15) and (12) into Eqs. (10) and (11), general equations with dependence on only a single dimension can be obtained:

$$R_s = \frac{\Delta R}{4\bar{R}} \sqrt{\frac{3000\bar{D}}{\chi(\bar{\lambda})w\langle v \rangle + 3\bar{D}}} \quad (16)$$

$$R_s = \frac{5\Delta\lambda}{2\bar{\lambda}} \sqrt{\frac{10\bar{D}}{8\bar{\lambda}^3w\langle v \rangle + \bar{D}}} \quad (17)$$

Eq. (16) is the most general model that includes all effects of interest in this work and should be compared to Eq. (11), which was used in earlier publications [21]. Note that Eq. (16) has the function $\chi(\lambda)$ embedded in it still (Eq. (7)) and that R and λ are also functions of w . These equations will provide a basic framework around which the various scaling effects associated with FFF systems can be compared.

4.3.1. EIFFF system modeling

As the particle-wall interaction induced exclusion layer could be a limiting factor on the extent to which FFF systems can be practically miniaturized, modeling results including the effect of a constant exclusion layer will be discussed first. In addition, geometric dimensions can have a significant impact on retention in EIFFF, so the mathematical models were explored to determine the impact of geometric changes on retention with resolution as the basis for the model comparison.

4.3.1.1. Model comparisons. Fig. 5 compares the effect of wall repulsion on resolution with a variation of channel height w . The modified λ , which includes the exclusion parameter calculated using Eq. (3) results in a modified retention ratio with a clear loss in the magnitude of the achievable resolution. It is important

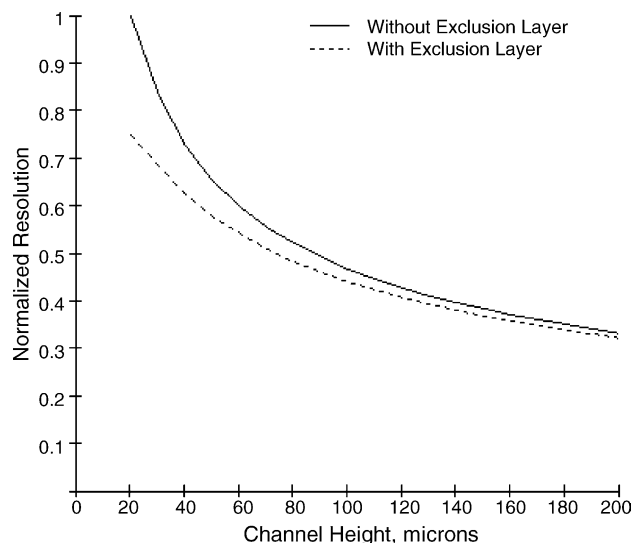


Fig. 5. Plots showing the effect of the particle-wall repulsion induced exclusion zone on resolution for the EIFFF system scaling model.

to note that the resolution trends remain the same with inclusion of the wall repulsion parameter.

Fig. 6 shows typical curves indicating the dependence of resolution on plate separation distance, w , for an EIFFF system. The upper two traces correspond to Eqs. (10) and (11) showing what appears to be only a small difference between these two equations. Closer inspection reveals that the smaller w becomes, the greater the difference between the equations. The calculations show that Eq. (11) would underestimate the theoretical resolution possible in a EIFFF channel by a minimum of 20% for the whole range of channel heights from 10 to 200 μm , confirming the value of more precise mathematical models. Also, resolution increases with a decrease in w , which is the established motivating factor for miniaturization of EIFFF systems [15]. For the typical inputs used in these equations, resolution

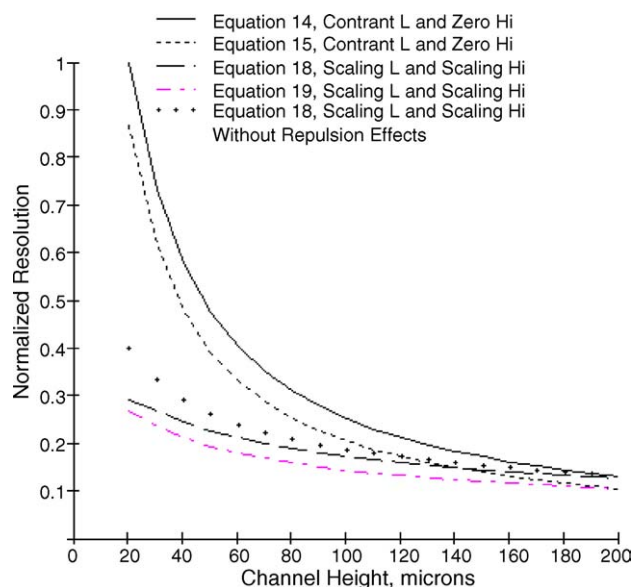


Fig. 6. Plots comparing the geometric scaling models for EIFFF system. Note that the constant length used for the simulation in this paper is 60 cm.

is nine times higher with a 10-fold reduction in channel height, and resolution increases with miniaturization for all models, but there is a distinct difference between resolutions estimated by the general model (Eq. (10)) and the simplified model (Eq. (11)) used in earlier papers [26]. The lowest two traces in Fig. 6 are plots of the estimated resolution when both H_i and L are scaled with w according to Eqs. (16) and (17). Once all the effects are included, the two equations appear to be offset from each other. Interestingly, this means that the error for the approximate equation, Eq. (17), is about 20% at small values of w , but is more than 25% as w reaches 200 μm , a substantial difference between the two models. The middle dotted trace is the plot of resolution variation according to Eq. (16) with scaling H_i and L , but without the wall repulsion parameter adjustment for λ . Ignoring the wall repulsion effect clearly results in overestimation of resolution and therefore wall repulsion needs to be accounted for in the resolution calculation.

The plots of Eqs. (11) and (16) indicate the differences between resolutions predicted by earlier publications and the general model that includes all relevant scaling effects. Note that both of these equations include the exclusion zone, which if not included in Eq. (11) would show an even more substantial difference between the two models. While the total resolution is significantly less in the general model, due to inclusion of H_i and reduced L , the overall trends remain the same, while giving a more accurate picture of the potential of miniaturization.

4.3.1.2. Instrumental plate height and length scaling. The two upper curves in Fig. 7 illustrate the effect of instrumental plate height on resolution for an EIFFF system and show that the difference due to a constant estimate of instrumental plate height and a scaling instrumental plate height is not significant except below 40 μm . The primary reasons for the differences were explained in Fig. 3 and are related to the relative importance of the instrumental and non-equilibrium plate heights as channel heights scale downward.

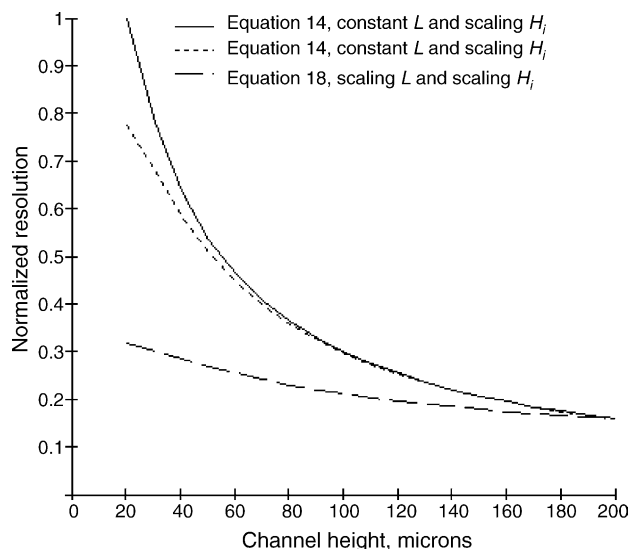


Fig. 7. Plots showing the effects of L and H_i scaling on the resolution of EIFFF system.

The data presented in the upper two traces of Figs. 6 and 7 ignore the reality that length will not remain constant for most systems as they are miniaturized, and a loss in resolution occurs as the channel length falls. The two lower curves in Fig. 6 and the lowest curve in Fig. 7, show the reduced gain in resolution that occurs as the channel length and the channel height scale proportionately and in accordance with Eq. (17). In order to achieve high-speed separations and gain the miniaturization related advantages described earlier, length will have to be reduced to an optimum determined by balancing the requirements of resolution and with limits on analysis time. EIFFF systems with a scaled length will be microsystems in the true sense, and to reflect this phenomenon in the theoretical analysis, length scaling according to Eq. (12) is included in the discussion on improved models in the remaining discussion.

The lowest trace in Fig. 7 represents the contribution of both a scaling length and a scaling plate height. The difference between this curve and the others indicates the impact of length on resolution, which is clearly significant. Large reductions in channel length are clearly detrimental to resolution, as expected, but are part of the tradeoffs that must be considered in channel design. As suggested by the discussion on Eq. (12), for systems where the field strength varies with w , L has a less significant impact on resolution than w , as indicated by the rise in resolution as w and L drop simultaneously.

Comparing all of the data from Figs. 6 and 7, it is clearly important to include L and H_i scaling in the model, and the use of more general models for the estimation of the channel function and for optimization of the instrument is justified.

4.3.2. General FFF system modeling

Unlike electrical and thermal FFF systems, mathematical models of general FFF systems predict a loss in resolution with miniaturization. Accordingly, miniaturization of such systems has not generally been attempted. The inclusion of instrumental plate height scaling, though, leads to potentially different conclusions.

The top trace in Fig. 8 is the simulation result for normalized resolution (Eq. (10)) where L and H_i are kept constant at 60 cm and 0 μm , respectively, which is the situation that is typically explored for miniaturization of general FFF systems. As expected, there is an almost 70% loss in resolution when w is scaled down from 200 to 20 μm , but the retention time is reduced by a factor of 10—an advantage at a heavy price.

Incorporation of the scaling effect associated with instrumental plate heights, though, reveals the possibility of a feasible miniature general FFF system. The bottom trace from Fig. 8 shows that when system parameters L and H_i scale with w , the resolution remains nearly constant and there is only an 8% loss in resolution when w is reduced from 200 to 10 μm , while the retention time is reduced 100 times (very high speed separations possible). This situation is the most likely one to be experienced in a practical situation, and provides evidence that miniaturization could be practical for general FFF systems [36].

Thus, a well-designed general FFF channel could show improvement in resolution with miniaturization due to the major improvements related to instrumental effects. Considering that

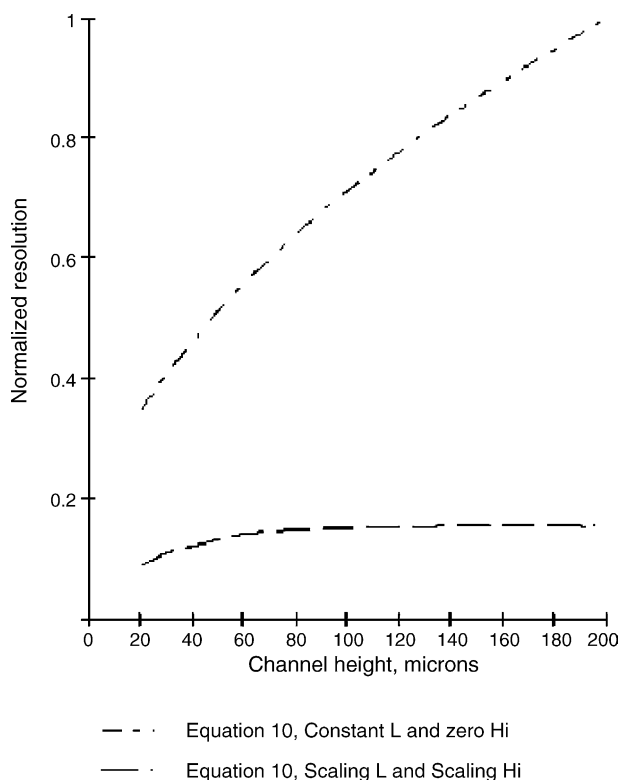


Fig. 8. Plot showing the effect of length and instrumental plate height on the resolution of general FFF systems.

there are several potential advantages from miniaturizing a general FFF system after a sensible trade-off between the analysis time and resolution is made, efforts to create these systems should be initiated. To gain all the advantages associated with miniaturization, though, general FFF systems may be required to operate under low retention conditions. The lower retention times associated with the high retention ratio will result in the reduced overall analysis time, while only sacrificing a small percentage of the potential resolution.

5. Conclusion

A linear reduction in instrumental plate heights with channel height is reported and it provides additional motivation for miniaturization of not only EIFFF systems, but also general FFF systems. In many cases, the instrumental plate height dominates the limit of operation of an FFF system, and thus a smaller system may have a significant advantage over larger versions. Accordingly, the theoretical role of geometry and other parameters that depend on geometry in FFF channels was investigated and show that miniaturization may be feasible for all FFF systems. Although scaling advantages for EIFFF are clear from the theory presented here and earlier publications, closer study of the scaling effects on EIFFF in the low retention regime revealed the need for improved scaling models for field flow fractionation systems so that optimization of the channel size can be performed. The proposed improved scaling models, which include an exclusion zone, instrumental plate height, and length effects, showed significant differences when compared to earlier

models. These improvements in accuracy could prove very critical for performance evaluation of a microsystem with highly controlled sample injection and an integrated on-chip detector. Further work will need to be done to verify the advantages associated with miniaturization in all FFF systems, and closer examination of electrical and thermal systems will be required to verify that there are no scaling effects associated with the applied fields and gradients. Also quantification of the repulsive forces in microsystem will have to be carried out to understand how the exclusion layer changes as channels are miniaturized, as it may limit the extent to which FFF systems can be miniaturized. With the possible role of field flow fractionation as the sample preparation component of a micro-total-analysis system becoming more probable; further efforts related to the performance of miniaturized systems should be completed.

Acknowledgements

This work was supported by NSF grant EPS-0092001, the United Engineering Foundation, the Whitaker Foundation, the Institute for Micromanufacturing at Louisiana Tech University, and the University of Utah.

References

- [1] T. Vilknér, D. Janáček, A. Manz, *Anal. Chem.* 76 (2004) 3373.
- [2] P. Auroux, D. Iossifidis, D. Reyes, A. Manz, *Anal. Chem.* 74 (2002) 2637.
- [3] J.C. Giddings, *Sep. Sci.* 1 (1966) 123.
- [4] J.C. Giddings, *Sep. Sci. Technol.* 19 (1984–1985) 831.
- [5] J.C. Giddings, F.J. Yang, M.N. Myers, *Science* 193 (1976) 1244.
- [6] G.H. Thompson, M.N. Myers, J.C. Giddings, *Anal. Chem.* 41 (1969) 1219.
- [7] J.C. Giddings, F.J.F. Yang, M.N. Myers, *Anal. Chem.* 46 (1974) 1917.
- [8] J.C. Giddings, M.N. Myers, *Sep. Sci. Technol.* 13 (1978) 637.
- [9] K.D. Caldwell, L.F. Kesner, M.N. Myers, J.C. Giddings, *Science* 176 (1972) 296.
- [10] J.C. Giddings, M. Martin, M.N. Myers, *Sep. Sci. Technol.* 14 (1979) 611.
- [11] G.H. Markx, R. Pethig, J. Rousselet, *J. Phys. D: Appl. Phys.* 30 (1997) 2470.
- [12] J.C. Giddings, *Anal. Chem.* 58 (1986) 2052.
- [13] T.M. Vickrey, J.A. Garcia-Ramirez, *Sep. Sci. Technol.* 15 (1980) 1297.
- [14] G. Liu, J.C. Giddings, *Anal. Chem.* 63 (1991) 296.
- [15] B.K. Gale, K.D. Caldwell, A.B. Frazier, *IEEE Trans. Biomed. Eng.* 45 (1998) 1459.
- [16] A.I.K. Lao, D. Trau, I.M. Hsing, *Anal. Chem.* 74 (2002) 5364.
- [17] T.L. Edwards, B.K. Gale, A.B. Frazier, *Anal. Chem.* 74 (2002) 1211.
- [18] J. Janca, I.A. Ananieva, A.Y. Menshikovab, T.G. Evseevab, J. Dupak, *J. Chromatogr. A* 1046 (2004) 167.
- [19] J. Yang, Y. Huang, X.-B. Wang, F.F. Becker, P.R.C. Gascoyne, *Anal. Chem.* 71 (1999) 911.
- [20] N. Tri, K. Caldwell, R. Beckett, *Anal. Chem.* 72 (2000) 1823.
- [21] B.K. Gale, K.D. Caldwell, A.B. Frazier, *Anal. Chem.* 73 (2001) 2345.
- [22] J.C. Giddings, *J. Microcol. Sep.* 5 (1993) 497.
- [23] B.K. Gale, A.B. Frazier, in: *Proceedings of the SPIE—The International Society for Optical Engineering, Society of Photo-Optical Instrumentation Engineers*, Bellingham, WA, USA, 1999, p. 190.
- [24] B.K. Gale, K.D. Caldwell, A.B. Frazier, *Anal. Chem.* 74 (2002) 1024.
- [25] H.J. Sant, B.K. Gale, in: *Proceedings of 9th International Symposium on Field-Flow Fractionation*, Boulder, CO, 2001.

- [26] G. Beecher (Ed.), *Research Instrumentation for the 21st Century*, Dordrecht, Martinus, Nijhoff Publishers, Netherlands, 1987, p. 89.
- [27] M.E. Schimpf, in: M.E. Schimpf, K.D. Caldwell, J.C. Giddings (Eds.), *Field-Flow Fractionation Handbook*, Wiley-Interscience, New York, NY, 2000, p. 95.
- [28] J.C. Giddings, *J. Chem. Phys.* 49 (1968) 81.
- [29] B.W. Rossiter, J.F. Hamilton (Eds.), *Physical Methods of Chemistry*, vol. IIIB, John Wiley and Sons, New York, NY, 1989.
- [30] J.M. Davis, in: M.E. Schimpf, K.D. Caldwell, J.C. Giddings (Eds.), *Field-Flow Fractionation Handbook*, Wiley-Interscience, New York, NY, 2000, p. 49.
- [31] J.C. Giddings, *J. Chem. Phys.* 49 (1968) 81.
- [32] M.E. Schimpf, in: M.E. Schimpf, K.D. Caldwell, J.C. Giddings (Eds.), *Field-Flow Fractionation Handbook*, Wiley-Interscience, New York, NY, 2000, p. 71.
- [33] J.C. Giddings, Y.H. Yoon, K.D. Caldwell, M.N. Meyers, M.E. Hovingh, *Sep. Sci.* 10 (1975) 447.
- [34] A.S. Said, *Theory and Mathematics of Chromatography*, Dr. Alfred Huethig Publishers, Heidelberg, Germany, 1981.
- [35] B.K. Gale, R.S. Besser, I. Papautsky, J.D. Brazzle, A.B. S Frazier, *Proceedings of the Advanced Technology Workshop (ATW) for MEMS and Microsystem Packaging and Integration*, 10–12 November 2000, Orlando, FL, 2000.
- [36] D. Kang, M. Moon, *Anal. Chem.* 76 (2004) 3851.